smoothly onto the front face shoulders of the main body, thereby converting the bluff body into an equivalent streamlined body to result in low drag. The drag touches the minimum at the optimum conditions.

Conclusions

The experiments with two bluff bodies placed in tandem showed an impressive drag reduction at optimum conditions. The square-plate front body resulted in a maximum of 80% drag reduction. The D-shaped front body was less effective in reducing the drag compared with the square-plate front body.

References

[1]Hoerner, S. F., *Fluid Dynamic Drag,* NJ, 1965.

[2]Morel, T., and Bohn, M., "Flow over Two Circular Disks In Tandem," *Transactions of the American Society of Mechanical Engineers, Journal of Fluids Engineering,* Vol. 102, March 1980, pp. 104–111.

[3]Koenig, K., and Roshko, A., "An Experimental Study of Geometrical Effects on the Drag and Flow Field of Two Bluff Bodies Separated by a Gap," *Journal of Fluid Mechanics,* Vol. 156, July 1985, pp. 167–204.

[4]Pamadi, B. N., Pereira, C., and Gowda, B. H. L., "Drag Reduction by Strakes of Noncircular Cylinders," *AIAA Journal,* Vol. 26, No. 3, 1986, pp. 292–299.

[5]Castro, I. P., and Robins, A. G., "The Flow Field Around a Surface Mounted Cube in Uniform and Turbulent Stream," *Journal of Fluid Mechanics,* Vol. 79, Pt. 2, 1977, pp. 307–335.

[6]Ogava, Y., and Oikava, S., "A Field Investigation of the Flow and Diffusion Around a Model Cube," *Atmospheric Environment,* Vol. 16, No. 2, 1982, pp. 207–222.

[7]Gowda, B. H. L., Gerhardt, H. J., and Kramer, C., "Surface Flow Field Around Three-dimensional Bluff Bodies," *Journal of Wind Engineering and Industrial Aerodynamics,* Vol. 11, 1983, pp. 405–420.

[8]Khalid, M., Palaniappan, C. T., and Rathakrishnan, E., "Passive Device for Base Drag Reduction," *Proceedings of the 18th National Conference on Fluid Mechanics and Fluid Power,* Indone, India, 1991, pp. G25–G34.

[9]Gowda, B. H. L., and Sitheeq, M., "Effect of Interference on the Pressure Distribution on a Three-Dimensional Bluff Body in Tandem Arrangement," *Indian Journal of Technology,* Vol. 29, No. 1, 1991, pp. 1–8.

Subsonic/Transonic Cascade Flutter Using a Full-Potential Solver

Milind A. Bakhle,* T. S. R. Reddy,* and Theo G. Keith Jr.†
University of Toledo, Toledo, Ohio 43606

Introduction

AEROELASTIC stability in transonic flow has received considerable attention in recent years. It has been observed[1,2] that the flutter speed of swept wings undergoes a sharp drop in the transonic regime; this has been referred to as the transonic flutter dip. This phenomenon is not modeled by the classical linear (flat-plate) aerodynamic theory. Hence, many nonlinear analyses have been used to model transonic flutter. However, all of the transonic flutter dip studies have been restricted to isolated airfoils. The blade-to-blade interaction in cascades, which is generally believed to be destabilizing, has not been considered in these analyses.

In the present work, the nonlinear unsteady full-potential aerodynamic solver of Refs. 3 and 4 is used for cascade flutter calculations in subsonic/transonic flow. Although the solver is nonlinear, the amplitude of blade motions is restricted to small values in the actual calculations. This ensures that the unsteady results are in the linear range (linear in the amplitude of motion); this allows efficient linear analysis methods to be used in the calculations. It should be noted that the steady flowfield is nonlinear and may be mixed subsonic/supersonic with shocks. In the present work, a frequency-domain analysis is used to calculate the flutter boundary for a cascade of NACA 64A010 airfoils; this airfoil section has been studied extensively in isolated airfoil transonic flutter studies. A comparison is made between the flutter results for a cascade and an isolated airfoil.

Presented as Paper 92-2119 at the AIAA Dynamics Specialist Conference, April 16–17, 1992; received April 24, 1992; revision received Nov. 21, 1992; accepted for publication Dec. 30, 1992.

*Senior Research Associate, Department of Mechanical Engineering. Member AIAA.

†Distinguished University Professor, Department of Mechanical Engineering. Associate Fellow AIAA.

Analysis

The aeroelastic model used in the present flutter analysis consists of a typical section structural model and an aerodynamic model based on the two-dimensional full-potential equation. Each blade of a bladed disk is represented by a rigid typical section model with two degrees of freedom—plunging and pitching. The aerodynamic model is based on the unsteady, two-dimensional, full-potential equation. The governing equation for irrotational, isentropic flow written in conservative form is

$$\frac{\partial \rho}{\partial t} + \frac{\partial (\rho u)}{\partial x} + \frac{\partial (\rho v)}{\partial y} = 0 \tag{1}$$

where

$$u = \frac{\partial \phi}{\partial x}, \qquad v = \frac{\partial \phi}{\partial y}$$

and

$$\frac{\rho}{\rho_\infty} = \left\{1 + \frac{(\gamma-1)}{2}\left[M_\infty^2 - \left(2\frac{\partial \phi}{\partial t} + [u^2+v^2]\right)\Big/ a_\infty^2\right]\right\}^{1/(\gamma-1)}$$

In the above, ρ is the fluid (air) density, u and v the fluid velocity components in the x and y directions, ϕ the velocity potential, a the sonic velocity, and M the Mach number. The governing equation is transformed to the computational plane where it is discretized and solved using a finite volume scheme. The solution is obtained using a time-marching algorithm that uses approximate factorization at each time level with quasi-Newton iterations to maintain time accuracy. The method of solution is described in detail in Refs. 3 and 4.

For a frequency-domain flutter analysis, frequency-domain aerodynamic coefficients are required for plunging and pitching motions of specified frequency and specified interblade phase angle for a given cascade geometry and steady flow condition. These coefficients are calculated efficiently using the combined pulse response and influence coefficient method described in Ref. 5.

Results and Discussion

Unsteady Aerodynamics

To verify the calculation of frequency-domain aerodynamic coefficients in transonic flow, comparisons have been made between results from the present method and those from a linearized potential method[6]; these comparisons can be found in Ref. 7. In general, good agreement is seen between the corresponding results. However, significant differences are seen for the following calculation: an unstaggered cascade of single-circular-arc airfoils with a gap-to-chord ratio of 1.0, with a thickness-to-chord ratio of 0.05, and a steady flow Mach number of 0.76 at the far upstream and downstream locations. The reduced frequency of pitching is 1.0 based on the airfoil chord and the interblade phase angle is 180 deg.

Since the present calculations are restricted to small amplitude motions, the present analysis is comparable to the linearized potential calculations of Ref. 6. Any differences in the results must be attributed to differences in the numerical scheme, boundary conditions, and discretization. Efforts are underway to isolate and eliminate these differences. A comparison of the unsteady pressure distribution is shown in Fig. 1 to demonstrate that both results are qualitatively similar. These results were obtained using a 61×31 grid with 61 points in the streamwise direction and 31 points in the direction of the stagger line in each blade passages; 31 points are

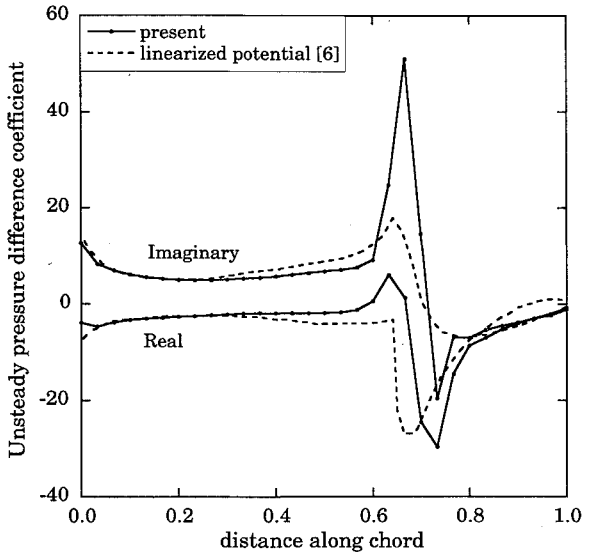

Fig.1 Comparison of pressure distribution with linearized potential theory.[6]

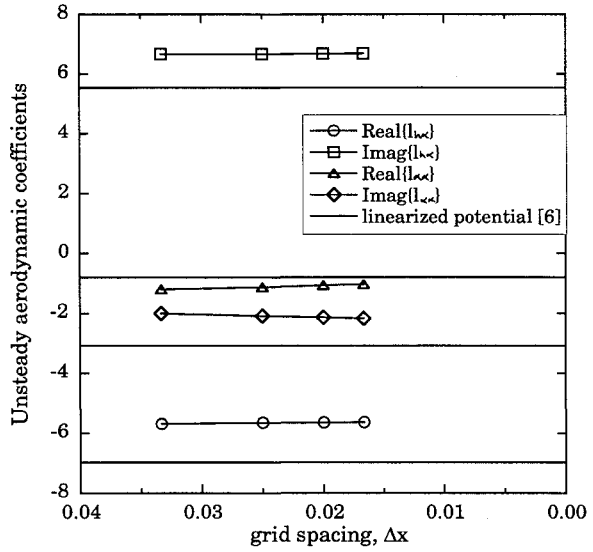

Fig.2 Effect of grid spacing on unsteady lift and moment coefficients ($l_{h\alpha}$ and $l_{\alpha\alpha}$).

located on each (upper and lower) surface of each airfoil; all grid points are uniformly distributed.

A grid-refinement study was performed to demonstrate that the present results do not change significantly with grid spacing. In the context of transonic flow, a refinement of the grid leads to a sharper capture of the shock and a higher pressure peak. However, the integrated force quantities such as lift and moment do not change substantially. Figure 2 shows the variation of unsteady lift and moment due to pitching, $l_{h\alpha}$ and $l_{\alpha\alpha}$, respectively, with grid spacing. Results are shown for four grids: 61×31, 81×41, 101×51, and 121×61 with spacings of Δx=0.033, 0.025, 0.020, and 0.067, respectively. The results from linearized potential theory are also included in Fig. 2; since these calculations are performed on a grid with variable spacing, the corresponding results are shown as lines instead of symbols. The calculations in Ref. 6 have been performed with a composite mesh consisting of a 62×20 global mesh and a 61×11 local mesh.

Flutter

Flutter results are presented for a cascade of NACA 64A010 airfoils; the airfoil section and structural parameters used here have been previously considered by several researchers in the isolated airfoil transonic flutter literature. In the present calculations, the cascade has eight blades; it is unstaggered and the gap-to-chord ratio is 1.0. The structural model for each blade is a two-degrees-of-freedom typical section with the elastic axis located a semichord upstream of the leading edge. This location of the elastic axis was chosen in Ref. 1 to simulate the dynamic characteristics of the tip section of a swept wing. The mass ratio is μ=60, the radius of gyration is r_α=1.8655, the offset between elastic axis and center of mass is x_α=1.8, and the ratio of uncoupled natural frequencies in bending and torsion is ω_h/ω_α=1.0.

Calculations have been performed using eight blade passages with a 61×21 grid in each passage; the number of grid points on each airfoil surface (upper and lower) is 31. Flutter calculations have been done for all of the eight different interblade phase angles at which flutter can occur for this cascade (σ=0, 45, 90 deg, etc.). It is found that σ=45 deg is the most unstable phase angle whereas σ=0 deg is the most stable; the remaining phase angles fall between these and are all nearly equally stable.

Figure 3 shows the variation of flutter reduced velocity V_f^* with Mach number M_∞ for an interblade phase angle of σ=45 deg. Calculations at M_∞=0.68 were not possible due to numerical difficulties; in this case, it was observed that after the transients (due to the pulse motion) had decayed, the flowfield did not return to the original undisturbed state. The results in Fig. 3 show that the flutter reduced velocity decreases continuously as the Mach number is increased until the flow is choked. However, when the shock is at the trailing edge (M_∞=0.7), the flutter speed increases with Mach number. A distinct difference is seen in the flutter results for choked and unchoked flows.

Transonic Dip Comparison

In Fig. 3, the present flutter results are compared with results from isolated airfoil calculations.[1] The cascade results are for σ=45 deg, which was found to be the most unstable phase angle. The isolated airfoil results taken from Ref. 1 have been obtained from a transonic small disturbance analysis. It can be seen that the flutter speed variations predicted by the present analysis are very similar to those from the isolated airfoil calculations. Three notable differences can be seen. First, the present results are translated along the Mach number axis (toward lower values) as compared to the isolated airfoil results. Second, the flutter velocity curve from the isolated airfoil calculations reaches higher values. Third, the present results show a clear increase in flutter velocity after the shock has reached the trailing edge; this is not seen in the isolated airfoil results.

To correlate the present results with the results from isolated airfoil calculations, a comparison of the corresponding steady flowfields follows. In the present calculations, the flowfield is entirely subsonic at initial Mach numbers below 0.68. At M_∞=0.68, a shock exists near the midchord of the airfoil; as the Mach number is increased, this shock moves downstream towards the trailing edge. For Mach numbers between 0.7 and 0.75, a fish-tail shock pattern exists at the trailing edge of the airfoils. Note that since the NACA airfoil is uncambered and the cascade is unstaggered, the steady flow over the upper and lower surfaces of the airfoil is iden-

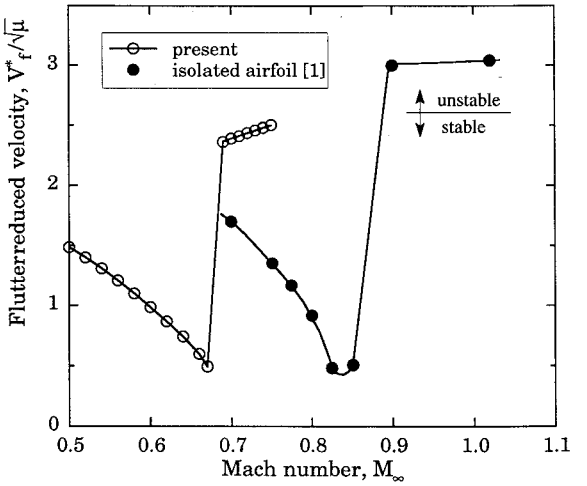

Fig.3 Flutter velocity for NACA 64A010 cascade at σ=45 deg.

tical. In Ref. 1, the following description of the steady flowfield is presented for the isolated airfoil. The flow is completely subsonic at Mach numbers below $M_\infty = 0.775$. A weak shock wave exists around midchord at $M_\infty = 0.8$; the shock is at the three-quarter chord point at $M_\infty = 0.85$. At $M_\infty = 0.9$, the fish-tail shock pattern appears.

Thus, it can be seen that some of the flow characteristics are similar in the cascade and isolated airfoil steady results. The shock is at the midchord location when $M_\infty = 0.68$ for the cascade and $M_\infty = 0.8$ for the isolated airfoil. Taking into account this difference, it can be seen that the present results are almost identical to the isolated airfoil results. However, note that the shock reaches the trailing edge at $M_\infty = 0.7$ in the cascade whereas for the isolated airfoil the corresponding value is $M_\infty = 0.9$. This shows that the shock location changes more rapidly in the cascade as the Mach number is changed from 0.68 to 0.7. Furthermore, the choking observed in the present cascade flow has no corresponding feature in isolated airfoil flow. Thus, although many similarities can be observed between the cascade results and the isolated airfoil results, distinct differences remain.

Concluding Remarks

Flutter calculations have been performed for an unstaggered NACA 64A010 cascade using the frequency-domain method. A comparison of the present results with isolated airfoil theory based on a transonic small-disturbance analysis shows that the flutter results are similar. The significant difference is a shift in the flutter velocity variation along the Mach number axis. It is concluded that the significant phenomena that lead to the distinct variations in flutter speed are present in both the isolated airfoil and cascade flows. However, a distinct difference between the two flows is the choking of the flow in the cascade. Because of this difference, a complete quantitative correlation of the two results is not expected.

References

[1]Isogai, K., "Numerical Study of Transonic Flutter of a Two-Dimensional Airfoil," National Aerospace Lab., Tokyo, Japan, NAL-TR-617T, July 1980.

[2]Isogai, K., "On the Transonic-Dip Mechanism of Flutter of a Sweptback Wing," *AIAA Journal*, Vol. 17, No. 7, 1979, pp. 793–795.

[3]Kao, Y. F., "A Two-Dimensional Unsteady Analysis for Transonic and Supersonic Cascade Flows," Ph.D. Thesis, School of Aeronautics and Astronautics, Purdue Univ., West Lafayette, IN, May 1989.

[4]Bakhle, M. A., Reddy, T. S. R., and Keith, T. G., Jr., "Time-Domain Flutter Analysis of Cascades Using a Full-Potential Solver," *AIAA Journal*, Vol. 30, No. 1, 1992, pp. 163–170.

[5]Bakhle, M. A., Mahajan, A. J., Keith, T. G., Jr., and Stefko, G. L., "Cascade Flutter Analysis with Transient Response Aerodynamics," *Computers and Structures*, Vol. 41, No. 5, 1991, pp. 1073–1085.

[6]Verdon, J. M., and Caspar, J. R., "A Linear Aerodynamic Analysis for Unsteady Transonic Cascades," NASA CR-3833, Sept. 1984.

[7]Bakhle, M. A., Reddy, T. S. R., and Keith, T. G., Jr., "An Investigation of Cascade Flutter Using a Two-Dimensional Full-Potential Solver," AIAA Paper 92-2119, April 1992.

Supersonic Panel Flutter Analysis of Shallow Shells

Maher N. Bismarck-Nasr*
Instituto Tecnológico de Aeronáutica,
São José dos Campos, SP, 12228-900, Brazil

I. Introduction

FLUTTER characteristics determination of shallow shells is of prime importance in supersonic aircraft and launch vehicle designs. The first analytical research on supersonic flutter of thin cylindrically curved panels was made by Voss,[1] using Reissner's shallow shell equations,[2] quasistatic aerodynamic theory, and the Galerkin method for the solution of freely supported ends boundary conditions. Nonlinear flutter analysis of two-dimensional[3] and three-dimensional[4] curved panels were performed by Dowell using a quasistatic aerodynamic theory. Dowell's investigations showed that the in-plane edge restraints had a great influence on the flutter boundaries, and this phenomenon was attributed to the frequency spectrum of the shells analyzed. Since Olson[5] introduced the aerodynamic matrix concept, many authors exploited the application of the finite element method in the field of supersonic panel flutter.[6] Reissner's two field variables principle[7] with transverse displacement and Airy stress functions taken as field variables represents an efficient alternative for the treatment of shallow shell problems. In spite of the simplifications it introduces, Reissner's principle is scarcely used in finite element formulation. The main reason is attributed to the difficulties encountered when applying the boundary conditions on Airy stress function.[8-9] In Ref. 10, starting from Reissner's variational equation for the free vibration of cylindrically curved panels, the Euler-Lagrange equations and the boundary conditions of the problem were deduced. It was shown that the boundary conditions on Airy stress functions are as simple and direct to apply as on the transverse displacements. The purpose of the present work is to present a finite element analysis of the supersonic flutter of cylindrically curved panels based on Reissner's two field variational principle.

II. Problem Formulation

The variational equation of thin cylindrically curved shallow shells,[7] Fig. 1., reads

$$\delta(\Pi^*) = \delta\left\{\frac{1}{2}\int_A \rho h w_{,t}^2\, dA - \frac{D}{2}\int_A [w_{,xx}^2 + w_{,yy}^2 + 2\nu w_{,xx}w_{,yy} + 2(1-\nu)w_{,xy}^2]\, dA + \frac{1}{2Eh}\int_A [F_{,xx}^2 + F_{,yy}^2 - 2\nu F_{,xx}F_{,yy} + 2(1+\nu)F_{,xy}^2]\, dA - \int_A \frac{w}{R}F_{,xx}\, dA + \int_A w\Delta p\, dA\right\} = 0 \quad (1)$$

In Eq. (1), ρ is the material mass density per unit of area, h is the shell thickness, $D = Eh^3/12(1-\nu^2)$ is the shell flexural rigidity, ν is Poisson's ratio, E is Young's modulus, and Δp is the aerodynamic pressure difference. Using the quasistatic aerodynamic theory, the relationship between Δp and w can be written as

$$\Delta p = -\frac{2Q}{\sqrt{M^2-1}}\frac{\partial w}{\partial x} \quad (2)$$

where $Q = \rho V^2/2$ is the dynamic pressure, M and V are the freestream Mach number and velocity, respectively. Performing the variational operation, grouping terms, and applying Green's theorem, the Euler-Lagrange equations of the problem are obtained and read

$$D\nabla^4 w + \frac{1}{R}F_{,xx} + \rho h w_{,tt} - \frac{2Q}{\sqrt{M^2-1}}w_{,x} = 0 \quad (3)$$

$$\nabla^4 F - \frac{Eh}{R}w_{,xx} = 0 \quad (4)$$

and the classical boundary conditions on an edge μ = constant, where μ stands for x or y, and η normal to μ direction are given by

Clamped edge $w = w_{,\mu} = 0$ and at a corner $F_{,\mu\eta} = 0$ (5a)

Free edge $F = F_{,\mu} = 0$ and at a corner $M_{,\mu\eta} = 0$

(i.e., $w_{,\mu\eta} = 0$) (5b)

Received July 28, 1992; revision received Dec. 17, 1992; accepted for publication Dec. 17, 1992.

*Professor, Division of Aeronautical Engineering. Member AIAA.